Molecular and Cellular Biomedical Sciences, Vol.9 No.3, November 2025, p.124-78
Print ISSN: 2527-4384, Online ISSN: 2527-3442
DOI: 10.21705/mcbs.v9i3.660

RESEARCH ARTICLE

MCBS
Mol Cell Biomed Sci. 2025; 9(3): 133-40
DOI: 10.21705/mcbs.v9i3.660

Hypoxia-Exosome Mesenchymal Stem Cells Therapy Reduces Interleukin-6 Levels and CD86 Expression

Adelia Bayu Isfandiari[1], Agung Putra[2,3,4], Eko Setiawan[1,5]

[1]*Department of Postgraduate Biomedical Science, Faculty of Medicine, Universitas Islam Sultan Agung, Semarang, Indonesia*
[2]*Stem Cell and Cancer Research (SCCR) Laboratory, Semarang, Indonesia*
[3]*Department of Pathological Anatomy, Faculty of Medicine, Universitas Islam Sultan Agung, Semarang, Indonesia*
[4]*Department of Doctoral Biomedical Science, Faculty of Medicine, Universitas Islam Sultan Agung, Semarang, Indonesia*
[5]*Department of Surgery, Faculty of Medicine, Universitas Islam Sultan Agung, Semarang, Indonesia*

Background: UVB exposure activates type 1 macrophages (CD86) and increases IL-6, both contributing to collagen loss. exosome hypoxia mesenchymal stem cells (EH-MSC) has anti-inflammatory properties, suggesting its potential role in modulating CD86 activation and IL-6 secretion. This study examines the effects of EH-MSC injections on CD86 and IL-6 levels in UVB-exposed skin with collagen loss.

Materials and methods: Experimental research post-test only control group design was conducted with 30 male Wistar rats (*Rattus norvegicus*, strain: Wistar Han) divided into five groups. G1: healthy rats, G2: UVB-exposed with a subcutaneous injection of 0.9% NaCl, G3: UVB-exposed with Hyaluronic Acid, and G4 & G5: UVB-exposed with EH-MSC injections of 200 µL and 300 µL, respectively. IL-6 and CD86 levels were analysed using ELISA and qRT-PCR at 14 days post-treatment continue with statistical analysis.

Results: IL-6 analysis showed that levels in G4 (107.70±47.86 pg/mL) and G5 (58.68±25.37 pg/mL) were notably lower than in G2 and G3 (p<0.05). Compared to G1 (32.28±14.65 pg/mL), G4 exhibited a statistically distinct increase (p<0.05), whereas G5 showed no significant difference (p>0.05). Meanwhile, CD86 data analysis showed that G4 (0.53±0.14 pg/mL) were lower than in G1 (1.03±0.01 pg/mL) and G2 (1.47±0.43 pg/mL), but not significantly different from G3 (0.87±0.1 pg/mL) and G5 (0.36±0.08 pg/mL). Similarly, CD86 expression in G5 decreased relative to G1 and G2 (p<0.05) but remained similar to G3 and G4.

Conclusion: EH-MSC injections (200 µL and 300 µL) significantly reduced IL-6 and CD86 levels in collagen loss rats, supporting its potential as a therapeutic approach for UVB-induced skin damage.

Keywords: *collagen loss, CD86, EH-MSC, IL-6, UVB*

Submission: February 16, 2025
Last Revision: March 19, 2025
Accepted for Publication: March 26, 2025

Corresponding Author:
Adelia Bayu Isfandiari
Department of Postgraduate Biomedical Science, Faculty of Medicine
Universitas Islam Sultan Agung
Terboyo Kulon, Semarang 50112, Indonesia
e-mail: adeliaisfandiari@gmail.com

Cell and Biopharmaceutical Institute

Introduction

Epidemiological studies show a global increase in various age groups of UVB-related skin problems including decreased collagen.[1] If left untreated, this will increase the risk of skin malignancies or melanoma. It is reported that there are 60 cases of melanoma every 100,000 people in a year in the fifth and sixth decades of age group. It has reported that exposure to UV light in childhood also increases the risk of melanoma in young adults more than threefold.[1]

Exposure to ultraviolet B (UVB) rays activates type 1 macrophages, marked by CD86 expression, and increases pro-inflammatory cytokines like Interleukin-6 (IL-6), both contributing to skin collagen loss.[2-4] Type 1 macrophages respond to UVB-induced skin damage and oxidative stress, releasing IL-6, a key inflammatory mediator.[5] Pro-inflammatory cytokines also stimulate matrix metalloproteinase (MMP), an enzyme degrading skin collagen. Decrease in the amount of collagen to the point of collagen loss occurs if the skin is continuously exposed to UVB rays over a certain period of time, resulting in a negative impact on a person's health and appearance. Exposure to UVB rays increases the production of reactive oxygen species (ROS) which causes oxidative stress and can damage the collagen structure, causing fine lines, wrinkles and decreased skin elasticity through the MAP kinase transduction pathway.[2,6] Apart from that, it can also cause deoxyribo nucleic acid (DNA) damage which causes skin cell death and produces side effects in the form of damage associated molecular patterns (DAMPs).[7,8] ROS together with DAMPs are able to stimulate the activation of local macrophages in the skin area to become type 1 macrophages. After being received by the toll-like receptor (TLR) type 1 macrophages, DAMP molecules are actively able to untie the NFkB-IKK complex which causes NFkB to become active, which will increase MMP, thereby triggering the transcription of pro-inflammatory cytokines, one of which is IL-6.[9,10]

The use of hyaluronic acid (HA) has become a common therapeutic option to treat collagen loss due to UVB exposure to the skin.[11-13] The HA molecule acts as an effective hydration agent to increase skin moisture and help maintain elasticity.[11-13] However, the therapeutic effects resulting from the use of HA are temporary. The use of HA requires repeated applications to maintain results.[14] This is caused by the inability of HA to suppress inflammation and free radicals which are a source of problems in collagen loss due to exposure to UVB rays. Treatment using other agents is still needed to produce a longer lasting effect to suppress inflammation that occurs in the skin layers due to exposure to UVB rays.

Exosome Hypoxia Mesenchymal Stem Cell (EH-MSC) content plays an important role in inhibiting type 1 macrophage polarization and IL-6 production in inflammatory conditions.[15-17] Micro ribonucleic acid (miRNA) molecules, namely miR-146a and miR-21 contained in EH-MSC is known to be able to inhibit type 1 macrophage activity and IL-6 production.[9,10,18] Exosomes contain anti-inflammatory cytokines such as Interleukin-10 (IL-10) which are able to suppress the release of the NFkB-IKK complex thereby preventing the transcription of inflammatory cytokines.[19-21] However, the role of EH-MSCs in inhibiting type 1 macrophage activation and IL-6 in mice models of collagen reduction due to UVB exposure has not been studied. This research aim to examines the effect of subcutaneous injection of EH-MSC in mice with a collagen loss model exposed to UVB on the expression of IL-6 and type 1 macrophages, especially CD86.

Materials and methods

Study Design

This study was conducted using a randomized post-test-only control group design to evaluate the effects of hypo-exo MSCs on IL-6 and CD68 levels in UV-B exposed Wistar rats. This experimental setup enabled a precise comparison between treated and untreated groups while minimizing potential bias. The study was approved by the Ethics Committee of the Faculty of Medicine, Universitas Islam Sultan Agung (No. 133/IV/2024/Komisi Bioetik).

MSC Cultures

All procedures were conducted in a class 2 biosafety cabinet (Esco, Cat. No. LA2-4A1, Singapore) using sterile equipment and strict sterility techniques. The umbilical cord was collected in transport medium, placed in a petri dish, and washed with PBS (Gibco, Cat. No. 20012068, Waltham, MA, USA). Blood vessels were removed, and the tissue was finely chopped and placed in a 25T flask. After adhering for 3 minutes to the flask surface, complete medium (DMEM [Gibco, Cat. No. 11965092, Waltham, MA, USA], fungizone [Gibco, Cat. No. 15290026, Waltham, MA, USA], penstrep [Gibco, Cat. No. 15140122, Waltham, MA, USA], FBS

Print ISSN: 2527-4384, Online ISSN: 2527-3442
DOI: 10.21705/mcbs.v9i3.660

[PAN-Biotech, Cat. No. P30-2602, Aidenbach, Germany]) was added. The flask was incubated at 37°C with 5% CO_2 (Thermo Fisher Scientific, Heracell VIOS 160i, USA). Cells appeared after approximately 14 days, and the medium was changed every 3 days. Once cells reached 80% confluency, they were passaged up to passage 4, and conditioned medium was collected at 70% confluency.

Isolation of MSCs-Derived Exosomes Hypoxia

Conditioned medium (passage 4) was centrifuged at 300×g for 5 minutes, then at 2000×g for 30 minutes to remove debris. The supernatant was filtered using tangential flow filtration (TFF) with 100 kDa and 500 kDa membranes (Millipore, Cat. No. Pellicon 2, Burlington, MA, USA). Exosomes were validated using flow cytometry markers CD81, CD63, and CD9 BD (Biosciences, Cat. No. 551108, 556019, and 555370, Franklin Lakes, NJ, USA), then stored in 2.5 mL vials at 2-8°C. MSCs at 80% confluency were placed in a hypoxic chamber (STEMCELL Technologies, Cat. No. 27310, Vancouver, Canada) with 10 mL of complete medium. Nitrogen gas was introduced until oxygen levels reached 5%, and the chamber was incubated at 37°C for 24 hours. The culture medium was then filtered using TFF, washed 2 times with stain buffer (PBS) (Gibco, Cat. No. 20012068, Waltham, MA, USA), and resuspended with 300-500 µL of stain buffer or 1-time washing buffer (FBS) (PAN-Biotech, Cat. No. P30-2602, Aidenbach, Germany). Tubes 1-5 were used as controls for setting up the cytometry (as compensation).

Animal Groups and Construction of a Collagen loss Model in Wistar Rats

All experiments were conducted using 2-3 month-old male Wistar rats (Rattus norvegicus, strain: Wistar Han, 200-250 grams) obtained from an accredited laboratory animal center. The animals were housed in standard conditions with a 12-hour light/dark cycle, controlled temperature (22-24°C), and ad libitum access to food and water. A total of 30 rats were divided into 5 groups. The first group (G1) was adapted for 7 days, and then 1 rat was taken to be validated macroscopically and microscopically. The other 24 rats were divided into 4 groups: G2, G3, G4, and G5. The G2 (negative control group) rats were exposed to UVB and received a subcutaneous injection of 200 µL of 0.9% NaCl solution. The G3 (control group) rats were exposed to UVB and received a subcutaneous injection of 200 µL of HA. The G4 (EH-MSC group) rats were exposed to UVB and received a subcutaneous injection of 200 µL of EH-MSC. The G5 (high-dose EH-MSC group) rats were exposed to UVB and received 300 µL of EH-MSC.

UVB light was irradiated on the rats' dorsal spine over a 2×3 cm area with a dose of 1 MED, at a distance of 20 cm for 8 minutes, 5 times a week, for 14 days. On the 15th day, 1 rat from each group was taken for macroscopic and microscopic validation. The remaining rats in each group were treated by subcutaneous injection. G2 was given 200 µL NaCl, G3 was given 200 µL hyaluronic acid, G4 was given 200 µL exosomes, and G5 was given 300 µL. After day 15, they were terminated using intramuscular ketamine (60 mg/kg, Sigma-Aldrich, USA) and xylazine (20 mg/kg, Sigma-Aldrich, USA). Blood samples of 0.5 mL were collected from the sinus orbita and immediately centrifuged at 15,000 rpm for 15 minutes at 4°C to obtain serum for IL-6 and CD86 level analysis.

Macroscopic and Microscopic Validation

Macroscopic validation was carried out to confirm clinically that UVB exposure was successful in creating a model of collagen loss in experimental animals. This involved direct visual examination of the skin to assess the presence of collagen damage, compared to rats not exposed to UVB (Figure 1).

Microscopic validation was carried out by histopathology using Masson Trichrome staining (Abcam, Cat. No. ab150686, Cambridge, UK). The tissue slides were deparaffinized, then incubated in heated Bouin's Fluid

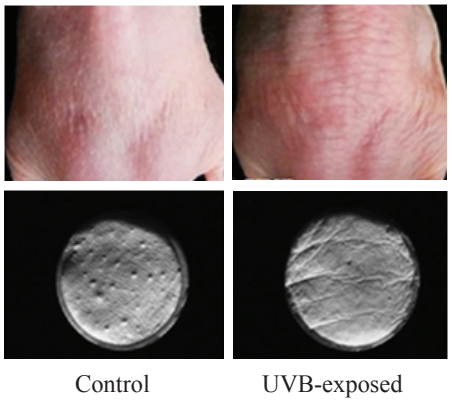

Figure 1. Validation in experimental animals involved assessing skin folds (wrinkles) and redness (erythematous) on the backs of rats exposed to UV light and those not exposed to UV light on the 14th day. Modified with permission.[22]

(Sigma-Aldrich, Cat. No. HT10132, St. Louis, MO, USA) at 54-64ºC for 60 minutes, followed by cooling for 10 minutes. After rinsing with running water, the slides were incubated in Weigert Iron Hematoxylin (Sigma-Aldrich, Cat. No. HT1079, St. Louis, MO, USA) for 5 minutes. After rinsing again with water, the slides were incubated in Biebrich Scarlet/Acid Fuchsin solution (Sigma-Aldrich, Cat. No. HT151, St. Louis, MO, USA) for 15 minutes, then rinsed with water. Next, the slides were incubated in phosphomolybdic/phosphotungstic acid solution (Sigma-Aldrich, Cat. No. HT153, St. Louis, MO, USA) for 10-15 minutes, followed by incubation in Aniline Blue solution (Sigma-Aldrich, Cat. No. HT152, St. Louis, MO, USA) for 5-10 minutes and rinsed with water. The slides were incubated in acetic acid solution for 3-5 minutes, then dehydrated and covered with a glass slide.

Analysis of IL-6 Levels by ELISA

The IL-6 analysis using ELISA began with sample preparation, followed by a blocking process to prevent nonspecific binding by covering empty areas on the microtiter plate (Corning, USA). The test samples (serum, plasma, or cell supernatant), along with positive and negative controls, were added and incubated to allow IL-6 to bind to the antibodies on the plate. The plate was then washed to remove unbound substances before adding specific detection antibodies against IL-6. An enzyme-conjugated antibody and a substrate were introduced to produce a color signal. The reaction was stopped, and the color intensity was measured using a spectrophotometer. Data analysis was performed by plotting absorbance values on a standard curve to determine IL-6 concentration in the samples

Analysis of CD86 Expression by Real Time PCR

Gene expression of CD86 was analyzed using reverse transcription-polymerase chain reaction (qRT-PCR). The PCR mixture consisted of 1 µL cDNA template, 10 µL of 2× SensiFAST SYBR No-ROX Mix, 0.8 µL forward primer, 0.8 µL reverse primer, and 7.4 µL NFW. The qRT-PCR process was carried out with an initial temperature of 95°C for 5 seconds, followed by 56°C for 20 seconds for 50 cycles. The hydrolyzed probe was analyzed at a wavelength of 520 nm. Quantification of qRT-PCR data was carried out using EcoStudy Software

Statistical Analysis

SPSS 26.0 (version 26.0; IBM Corp., Armonk, NY) was used for analysis. Normality and distribution tests were performed using the Shapiro-Wilk and Levene tests. If the data distribution was normal and homogeneous ($p>0.05$), the One-Way ANOVA test was used. If there was a significant difference ($p<0.05$), a post hoc test was carried out.

Results

EH-MSCs Exhibited Spindle Morphology and Expressed MSC-Specific Surface Markers

After reaching the fourth passage, EH-MSCs adhered to the bottom of the petri dish and exhibited spindle-shaped morphology under microscopic observation (Figure 2). Flow cytometry analysis confirmed high expression of MSC markers CD90 (100%) and CD29 (99.95%), with minimal expression of hematopoietic and endothelial markers CD45 (0.27%) and CD31 (0.32%). Although CD73 and CD105 were not assessed, the overall surface marker profile supported the classification of the cells as mesenchymal stem cells.

EH-MSCs Induced Osteogenic and Adipogenic Differentiation

EH-MSCs successfully induced osteogenic and adipogenic differentiation, as evidenced by calcium deposits stained with Alizarin Red and lipid droplets stained with Oil Red O in osteogenic and adipogenic cultures (Figure 3).

UVB Exposure Induced Collagen Loss in Rats

Macroscopic observations showed that UVB-exposed rats developed more prominent skin wrinkles compared to non-exposed controls (Figure 4). Histological analysis using Masson's Trichrome staining revealed a reduction in collagen density in UVB-exposed skin tissue. This confirmed that UVB exposure induced both visible and structural collagen degradation.

EH-MSC Treatment Reduced IL-6 Levels and CD86 Expression in UVB-Exposed Rats

Data analysis of IL-6 levels and CD86 expression was subjected to normality distribution analysis in each group. The Shapiro-Wilk test confirmed that IL-6 and CD86 data followed a normal distribution. Levene's test showed homogeneity for IL-6, while CD86 was non-homogeneous. IL-6 levels were analyzed using one-way ANOVA, followed by LSD post hoc test for pairwise comparisons. CD86 expression was analyzed using the Kruskal-Wallis test, followed by the Tamhane post hoc test. The administration of EH-MSC at 200 µL and 300 µL resulted in a notable

Print ISSN: 2527-4384, Online ISSN: 2527-3442
DOI: 10.21705/mcbs.v9i3.660

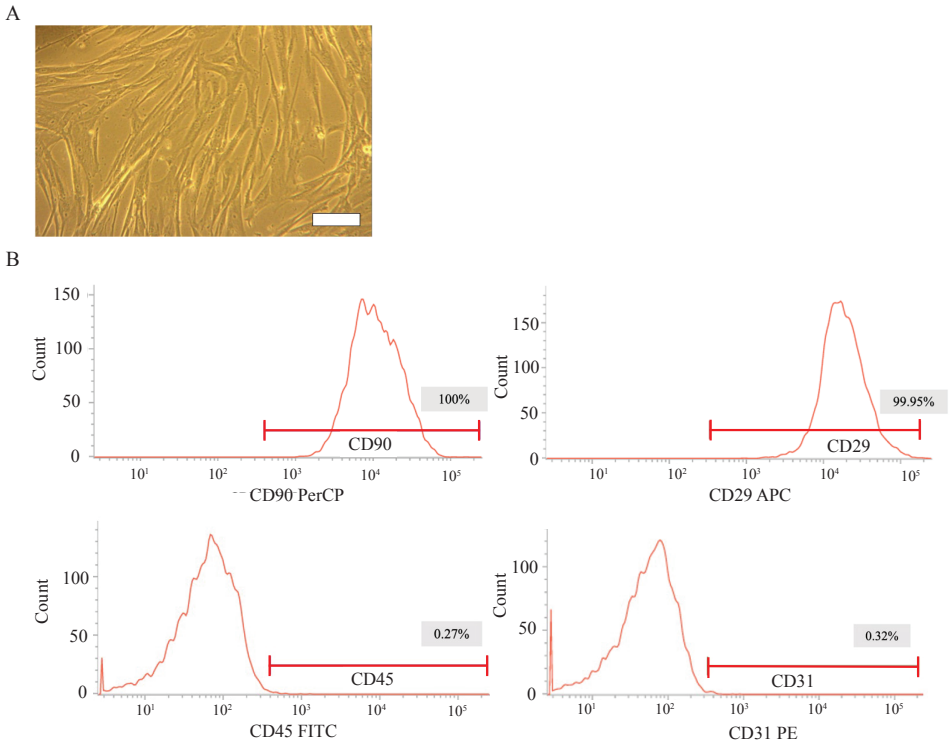

Figure 2. EH-MSCs Exhibited Spindle Morphology and Expressed MSC-Specific Surface Markers. A: MSC morphology is fibroblast-like at 40x magnification. B: Flow cytometry analysis of CD90, CD29, CD45, and CD31 expression. White bar: 100 µm.

reduction in IL-6 and CD86 expression compared to UVB-exposed controls. The results of IL-6 data analysis showed that G4 (107.70±47.86 pg/mL) and G5 (58.68±25.37 pg/mL) were significantly different compared to G2 and G3. However, when compared with G1 (32.28±14.65 pg/mL), G4 had significantly different IL-6 levels, while G5 was not significant .

Based on the results of data analysis, it was found that G4 (0.53±0.14) was significantly lower (p<0.05) compared to G1 (1.03±0.01) and G2 (1.47±0.43) and not significantly different when compared with G3 (0.87±0.1) and G5 (0.36±0.08) (Figure 5). The CD86 expression decreased significantly compared to G1 and G2 (p<0.05), but not significantly compared to G3 and G5.

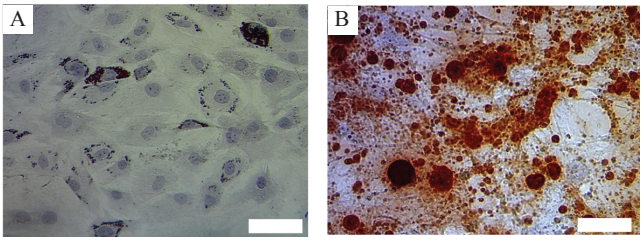

Figure 3. The ability of MSCs to differentiate into Adipocytes on oil red o staining (indicated by black arrows) (A) and Osteocytes on alizarin red staining (B). White bar: 100 µm.

Discussion

Research findings showed that both doses of EH-MSC injection succeeded in reducing IL-6 levels and CD86 expression. In addition, injection of EH-MSC with levels of 200 uL and 300 uL has a better ability to reduce IL-6 and CD86 expression when compared with HA. Apart from that, this study also found that injection of EH-MSC levels of 200 µL and 300 µL further reduced M1 activation so that M2 could increase when compared to HA. This shows that EH-MSC is more capable of inhibiting collagen loss.

Exosomes from MSCs have become an interesting research subject in regenerative therapy due to their potential in stimulating tissue regeneration and regulating immune responses. Among the components contained in these exosomes, miRNAs, growth factors, and cytokines play a key role in mediating the anti-inflammatory and immunomodulatory effects of MSCs. The miRNAs in exosomes can interact with certain gene targets in target cells, regulating the expression of genes involved in various biological processes, including inflammatory responses.[1,23] Meanwhile, growth factors in exosomes (EGF or FGF) can stimulate cell proliferation and differentiation target cells, as well as influencing signaling pathways involved in the immune response. In addition, pro-inflammatory cytokines found in exosomes, such as IL-6, can trigger a strong inflammatory response in pathological conditions.[24,25]

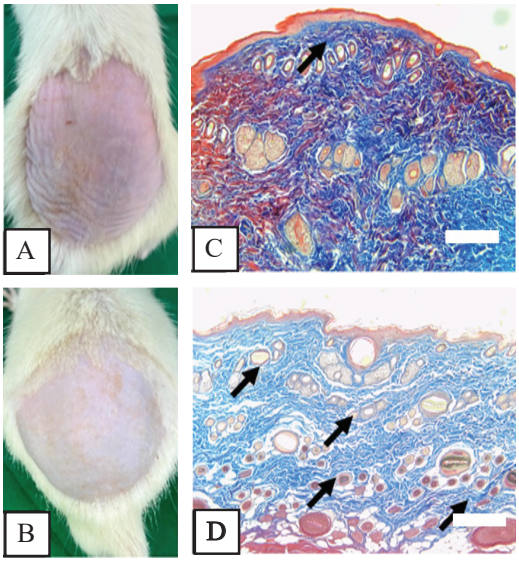

Figure 4. UVB Exposure Induced Collagen Loss in Rats. The skin of mice exposed to UVB looks more wrinkled (A) compared to skin that was not exposed to UVB (B). Less blue collagen (black arrow) is visible in the skin of mice exposed to UVB (C) compared to the skin of mice without UVB exposure (D). White bar: 100µm

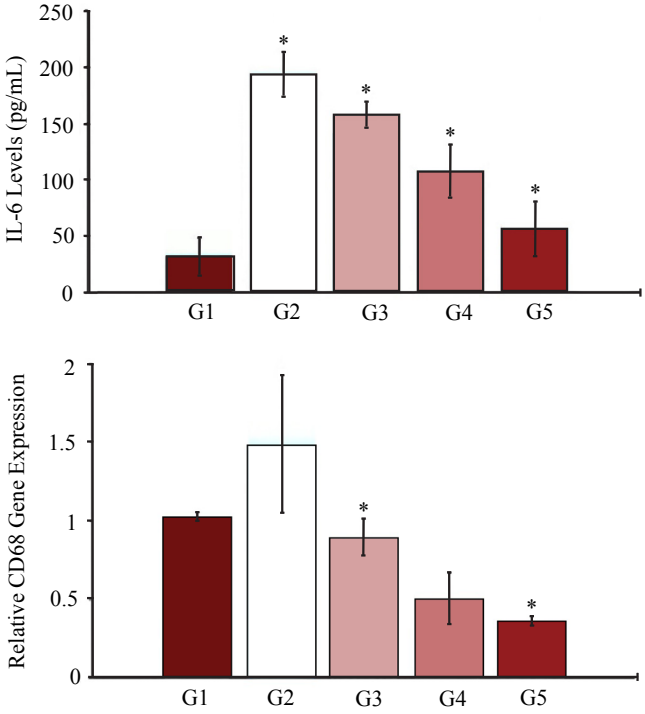

Figure 5. EH-MSC Treatment Reduced IL-6 Levels and CD86 Expression in UVB-Exposed Rats. G1: Control; G2: UVB+0.9% NaCL; G3: UVB+200 µL HA; G4: UVB+200 µL EH-MSC; G5: UVB+300 µL EH-MSC. *Significant compare to G2 group.

In the context of decreased IL-6 and inhibition of M1 (CD86) activation, MSCs exosomes can deliver miRNAs that can regulate the expression of certain genes in target cells, including genes involved in IL-6 production and macrophage polarization.[26] For example, certain miRNAs in exosomes can targets IL-6 mRNA, reducing its production and reducing the inflammatory response. In addition, exosomes also contain growth factors and cytokines that can modulate signaling pathways that regulate CD86 expression on macrophages, leading to inhibition of M1 activation and suppression of inflammatory responses.[27,28]

NF-kB pathway is one of the signaling pathways involved in regulating the expression of pro-inflammatory genes such as IL-6. MSCs exosomes can contain miRNAs that inhibit NF-κB activation, thereby reducing levels of IL-6 and other pro-inflammatory cytokines. Through NF-kB regulation, exosomes can also influence CD86 gene expression and lead to reduced M1 activation inhibition so that M2 increases in macrophages.[29,30] Besides NF-κB pathway, Nrf2 pathway may also be involved in the anti-inflammatory effects of MSCs exosomes. Activation of Nrf2 can produce anti-inflammatory effects through regulation of antioxidant and detoxification genes, which can reduce inflammatory responses and suppress M1 polarization in macrophages. MSCs can contain miRNAs or growth factors that can modulate Nrf2 activation, providing protection against tissue damage caused by excessive inflammation.[14]

Certain proteins in MSCs exosomes may also contribute to their anti-inflammatory and immunomodulatory effects. For example, heat shock proteins (HSP) in exosomes can protect target cells from oxidative stress and inflammation, reducing the production of IL-6 and other pro-inflammatory cytokines.[31,32] Additionally, proteins such as TSG-6 can inhibit NF-kB activation and reduces IL-6 production, as well as influencing macrophage polarization towards an anti-inflammatory phenotype. Thus, through a combination of miRNAs, growth factors, cytokines, and proteins contained in MSCs exosomes, reduction of IL-6 and inhibition of M1 polarization can be achieved, providing promising therapeutic potential for inflammatory conditions and diseases associated with excessive immune activation.[23,33]

This study did not examine specific protein markers such as PD-L1, CD9, and CD81, which could further clarify

Print ISSN: 2527-4384, Online ISSN: 2527-3442
DOI: 10.21705/mcbs.v9i3.660

the role of exosomes in immunomodulation. This study also focused on short-term effects (14 days), and long-term outcomes on collagen restoration and macrophage polarization require further investigation. Future research should explore higher EH-MSC doses, longer observation periods, and additional molecular markers to better understand the mechanism of action.

Conclusion

EH-MSCs have the potential to improve skin collagen loss, as evidenced by changes in interleukin 6 levels and CD86 expression, providing a theoretical basis for the clinical application of EH-MSCs in treating skin collagen loss.

Authors' Contributions

ABI, AP, and ES were involved in conceptualizing and planning the research. ABI performed data acquisition/collection, calculated the experimental data, analyzed the data, drafted the manuscript, designed the figures, and interpreted the results. ABI, AP, and ES contributed to the critical revision of the manuscript.

Conflict of Interest

The authors declare that they have no conflicts of interest or competing interests related to the content of this manuscript.

References

1. Shah K, Minkis K, Swary JH, Alam M. Photoaging. In: Draelos ZD, editor. Cosmetic Dermatology. Hoboken, NJ: Wiley; 2022. p.16-25.
2. Tang CH, Chen CF, Chen WM, Fong YC. IL-6 Increases MMP-13 expression and motility in human chondrosarcoma cells. J Biol Chem. 2011; 286(13): 11056-66.
3. Hiromi N, Nakano H, Matsuzaki Y, Sawamura D, Hanada K. Immunohistochemical analysis of in vivo UVB-induced secretion of IL-1α and IL-6 in keratinocytes. Mol Med Rep. 2011; 4(4): 611-4.
4. Park G, Qian W, Zhang MJ, Chen YH, Ma LW, Zeng N, *et al*. Platelet-rich plasma regulating the repair of ultraviolet B-induced acute tissue inflammation: Adjusting macrophage polarization through the activin receptor-follistatin system. Bioengineered. 2021; 12(1): 3125-36.
5. Sharma MR, Mitrani R, Werth VP. Effect of TNFα blockade on UVB-induced inflammatory cell migration and collagen loss in mice. J Photochem Photobiol B. 2020; 213: 112072. doi: 10.1016/j.jphotobiol.2020.112072.
6. Cai G, Cai G, Zhou H, Zhuang Z, Liu K, Pei S, *et al*. Mesenchymal stem cell-derived exosome miR-542-3p suppresses inflammation and prevents cerebral infarction. Stem Cell Res Ther. 2021; 12(1): 2. doi: 10.1186/s13287-020-02030-w. Retraction in: Stem Cell Res Ther. 2023; 14(1): 9. doi: 10.1186/s13287-022-03227-x.
7. Bu T, Li Z, Hou Y, Sun W, Zhang R, Zhao L, *et al*. Exosome-mediated delivery of inflammation-responsive Il-10 mRNA for controlled atherosclerosis treatment. Theranostics. 2021; 11(20): 9988-10000.
8. Duan J, Li Y, Gao J, Cao R, Shang E, Zhang W. ROS-mediated photoaging pathways of nano- and micro-plastic particles under UV irradiation. Water Res. 2022; 216: 118320. doi: 10.1016/j.watres.2022.118320.
9. Kartika R, Wibowo H. Impaired function of regulatory T cells in type 2 diabetes mellitus. Mol Cell Biomed Sci. 2020; 4(1): 1-9.
10. Aryana IGPS, Hapsari AAAR, Kuswardhani RAT. Myokine regulation as marker of sarcopenia in elderly. Mol Cell Biomed Sci. 2018; 2(2): 38-47.
11. Kleine-Börger L, Meyer R, Kalies A, Kerscher M. Approach to differentiate between hyaluronic acid skin quality boosters and fillers based on their physicochemical properties. J Cosmet Dermatol. 2022; 21(1): 149-57.
12. Espinoza L, Vinshtok Y, McCreesh J, Tyson J, McSorley M. Kinetic energy-assisted delivery of hyaluronic acid for skin remodeling in middle and lower face. J Cosmet Dermatol. 2020; 19(9): 2277-81.
13. Grégoire S, Man PD, Maudet A, Le Tertre M, Hicham N, Changey F, *et al*. Hyaluronic acid skin penetration evaluated by tape stripping using ELISA kit assay. J Pharm Biomed Anal. 2023; 224: 115205. doi: 10.1016/j.jpba.2022.115205.
14. Chircov C, Grumezescu AM, Bejenaru LE. Hyaluronic acid-based scaffolds for tissue engineering. Rom J Morphol Embryol. 2018; 59(1): 71-6.
15. Zhao C, Chen JY, Peng WM, Yuan B, Bi Q, Xu YJ. Exosomes from adipose derived stem cells promote chondrogenesis and suppress inflammation by upregulating miR 145 and miR 221. Mol Med Rep. 2020; 21(4): 1881-9.
16. Eshghi F, Tahmasebi S, Alimohammadi M, Soudi S, Khaligh SG, Khosrojerdi A, *et al*. Study of immunomodulatory effects of mesenchymal stem cell-derived exosomes in a mouse model of LPS induced systemic inflammation. Life Sci. 2022; 310: 120938. doi: 10.1016/j.lfs.2022.120938.
17. Kheirkhah AH, Shahcheraghi SH, lotfi M, lotfi M, Raeisi S, Mirani Z. Mesenchymal stem cell derived-exosomes as effective factors in reducing cytokine storm symptoms of COVID-19. Protein Pept Lett. 2021; 28(8): 945-52.
18. Yang H, Chen J. Bone marrow mesenchymal stem cell-derived exosomes carrying long noncoding RNA ZFAS1 alleviate oxidative stress and inflammation in ischemic stroke by inhibiting microRNA-15a-5p. Metab Brain Dis. 2022; 37(7): 2545-57.
19. Singla D, Johnson T, Tavakoli Dargani Z. Exosome treatment enhances anti-inflammatory M2 macrophages and reduces inflammation-induced pyroptosis in doxorubicin-induced cardiomyopathy. Cells. 2019; 8(10): 1224. doi: 10.3390/cells8101224.
20. Kim M, Shin D Il, Choi BH, Min BH. Exosomes from IL-1β-primed mesenchymal stem cells inhibited IL-1β- and TNF-α-mediated inflammatory responses in osteoarthritic SW982 cells. Tissue Eng Regen Med. 2021; 18(4): 525-36.
21. Chouw A, Triana R, Dewi NM, Darmayanti S, Rahman MN, Susanto A, *et al*. Ischemic stroke: New neuron recovery approach with mesenchymal and neural stem cells. Mol Cell Biomed Sci. 2018; 2(2): 48-54.
22. Kim HN, Gil CH, Kim YR, Shin HK, Choi BT. Anti-photoaging properties of the phosphodiesterase 3 inhibitor cilostazol in ultraviolet B-irradiated hairless mice. Sci Rep. 2016; 6(1): 31169.

doi: 10.1038/srep31169.

23. Sofyanti Putri R, Putra A, Chodidjah D, Masyitah Darlan D, Trisnadi S, Thomas S, *et al*. Clitorea ternatea flower extract induces platelet-derived growth factor (PDGF) and GPx gene overexpression in ultraviolet (UV) B irradiationinduced collagen loss. Med Glas. 2022; 20(1): 15-21.
24. Chandel NS, Trzyna WC, McClintock DS, Schumacker PT. Role of oxidants in NF-κB activation and TNF-α gene transcription induced by hypoxia and endotoxin. J Immunol. 2000; 165(2): 1013-21.
25. Yang YN, Wang F, Zhou W, Wu ZQ, Xing YQ. TNF-α stimulates MMP-2 and MMP-9 activities in human corneal epithelial cells via the activation of FAK/ERK signaling. Ophthalmic Res. 2012; 48(4): 165-70.
26. Mirastschijski U, Lupše B, Maedler K, Sarma B, Radtke A, Belge G, *et al*. Matrix metalloproteinase-3 is key effector of TNF-α-induced collagen degradation in skin. Int J Mol Sci. 2019; 20(20): 5234. doi: 10.3390/ijms20205234.
27. Norouzi-Barough L, Shirian S, Gorji A, Sadeghi M. Therapeutic potential of mesenchymal stem cell-derived exosomes as a cell-free therapy approach for the treatment of skin, bone, and cartilage defects. Connect Tissue Res. 2022; 63(2): 83-96.
28. Ha DH, Kim H keun, Lee J, Kwon HH, Park GH, Yang SH, *et al*. Mesenchymal stem/stromal cell-derived exosomes for immunomodulatory therapeutics and skin regeneration. Cells. 2020; 9(5): 1157. doi: 10.3390/cells9051157.
29. Zhang B, Wang M, Gong A, Zhang X, Wu X, Zhu Y, *et al*. HucMSC-exosome mediated-wnt4 signaling is required for cutaneous wound healing. Stem Cells. 2015; 33(7): 2158-68.
30. Wang X, Liu Y, He J, Wang J, Chen X, Yang R. Regulation of signaling pathways in hair follicle stem cells. Burns Trauma. 2022; 10: tkac022. doi: 10.1093/burnst/tkac022.
31. Nguyen Hong S, Dinh Huu N, Nguyen Duy N, Than Trong T, Nguyen Bac H, Nguyen Van T, *et al*. Serial excision for the treatment of giant congenital melanocytic nevus: The Vietnamese way. Maced J Med Sci. 2019; 7(2): 231-3.
32. Nejati S, Mongeau L. Injectable, pore-forming, self-healing, and adhesive hyaluronan hydrogels for soft tissue engineering applications. Sci Rep. 2023; 13(1): 14303. doi: 10.1038/s41598-023-41468-9.
33. Bashir MM, Sharma MR, Werth VP. UVB and proinflammatory cytokines synergistically activate TNF-alpha production in keratinocytes through enhanced gene transcription. J Invest Dermatol. 2009; 129(4): 994-1001.